Supporting Information

Wearable Triboelectric-Human-Machine-Interface (THMI) Using Robust Nanophotonic Readout

Bowei Dong,‡[ab] Yanqin Yang, ‡[ab] Qiongfeng Shi, ‡[ab] Siyu Xu, [ab] Zhongda Sun, [ab] Shiyang Zhu,[c] Zixuan Zhang, [ab] Dim-Lee Kwong, [c] Guangya Zhou, [bd] Kah-Wee Ang, [ab] and Chengkuo Lee[abe]*

[a] Department of Electrical and Computer Engineering, National University of Singapore, 4 Engineering Drive 3, Singapore 117576, Singapore

[b] Center for Intelligent Sensors and MEMS (CISM), National University of Singapore, 5 Engineering Drive 1 Singapore 117608, Singapore

[c] Institute of Microelectronics, Agency for Science, Technology and Research (A*STAR), 2 Fusionopolis Way Singapore 138634, Singapore

[d] Department of Mechanical Engineering, National University of Singapore, 9 Engineering Drive 1, Singapore 117575, Singapore

[e] NUS Graduate School for Integrative Sciences & Engineering (NGS), National University of Singapore, 21 Lower Kent Ridge Road, Singapore 119077, Singapore

*Corresponding Author: Chengkuo Lee: elelc@nus.edu.sg

Note S1 General working mechanism of the integrated system

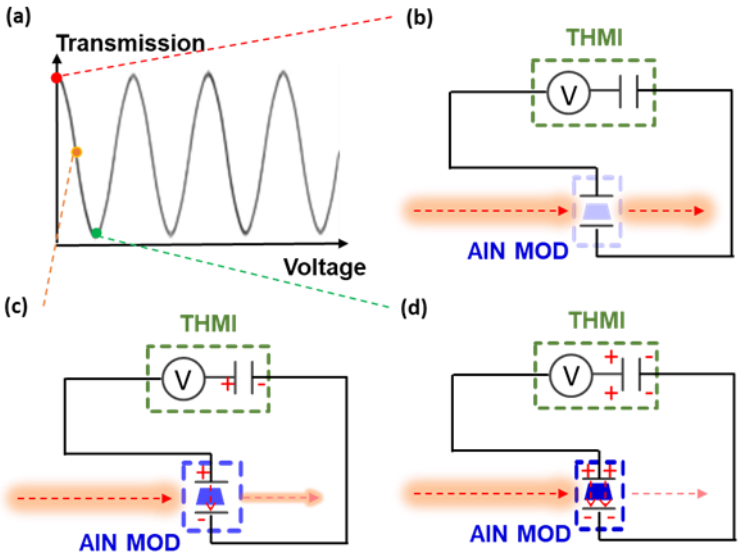

Figure S1. General working mechanism of the integrated system. (a) Transmission of a nanophotonic readout circuit as a function of THMI output voltage. The AlN modulator works at a wavelength with constructive interference. (b) Strong transmission when THMI provides zero voltage. (c) Weaker transmission when THMI provides a small voltage. (d) Negligible transmission when THMI provides a high voltage.

At a specific wavelength, the transmission of AlN modulator is determined by the voltage applied on the pair of top and bottom electrodes sandwiching the waveguide. The relation between the transmission and the applied voltage shows a sinusoidal waveform which is the feature of interferometers (Figure S2a). The modulation mechanism is the Pockels effect. Taking an example without loss of generality, the AlN modulator is originally working at a wavelength with constructive interference when the THMI provides zero voltage (Figure S1b). A small open-circuit voltage is applied to the AlN modulator when the THMI is slightly activated, leading to the

decrease of transmission (Figure S1c). With proper design, the transmission can be tuned to zero when the THMI provides a high voltage (Figure S1d).

In more general cases, the original transmission (the red dot shown in Figure S1a) can be arbitrarily chosen by operating the AlN modulator at different wavelengths. The final transmission after THMI's modulation can be controlled continuously by varying THMI's output voltage which is linked to the mechanical stimulation on the THMI. Thus, the output transmission can well reflect the mechanical stimulation of THMIs.

Note S2 Optical and tunneling electron microscope images of triboelectric-human-machine-interface-(THMI) and nanophotonic readout circuits

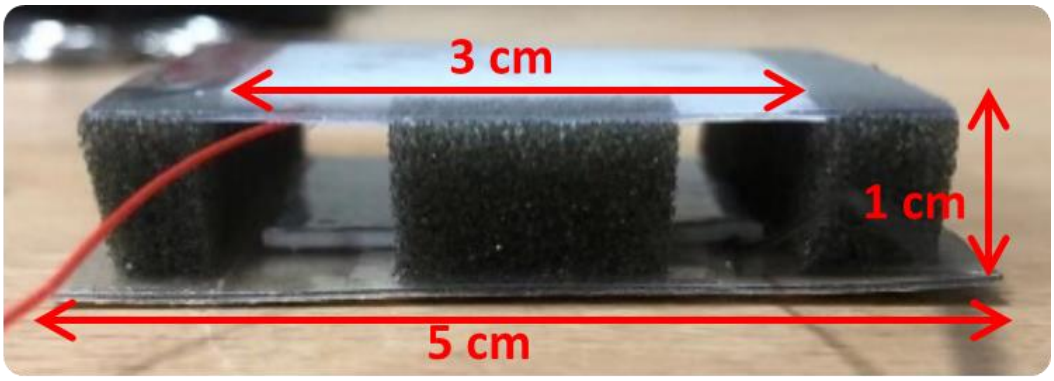

Figure S2. Optical image of the spacer triboelectric-human-machine-interface (S-THMI).

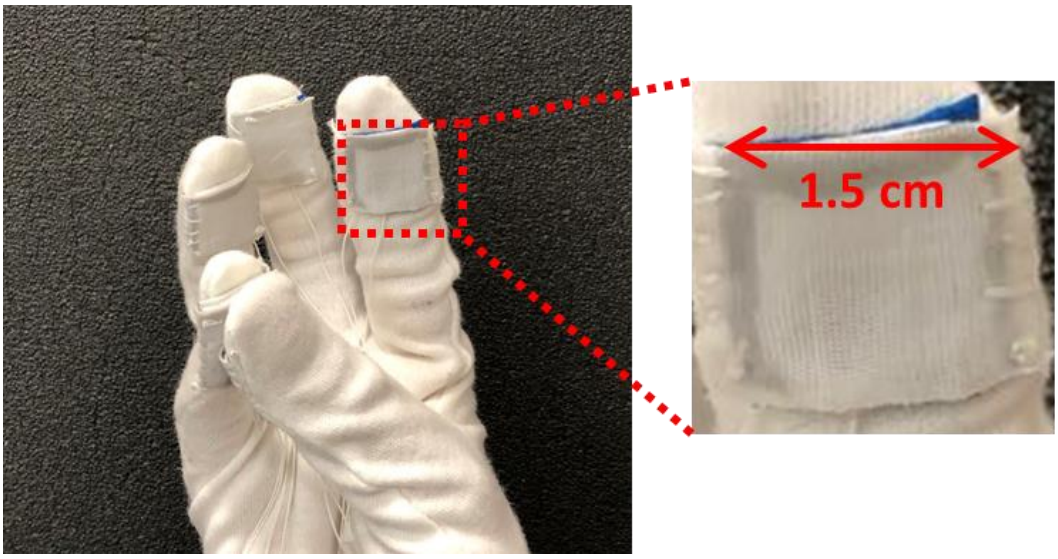

Figure S3. Optical images of the textile-human-machine-interface (T-THMI).

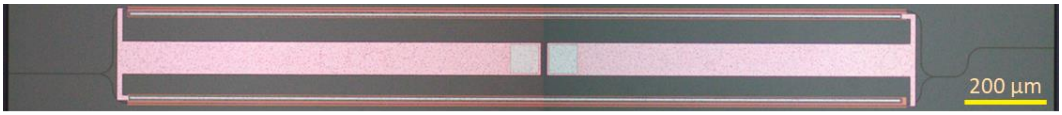

Figure S4. Optical microscope image of the short aluminum nitride (AlN) Mach-Zehnder interferometer (MZI).

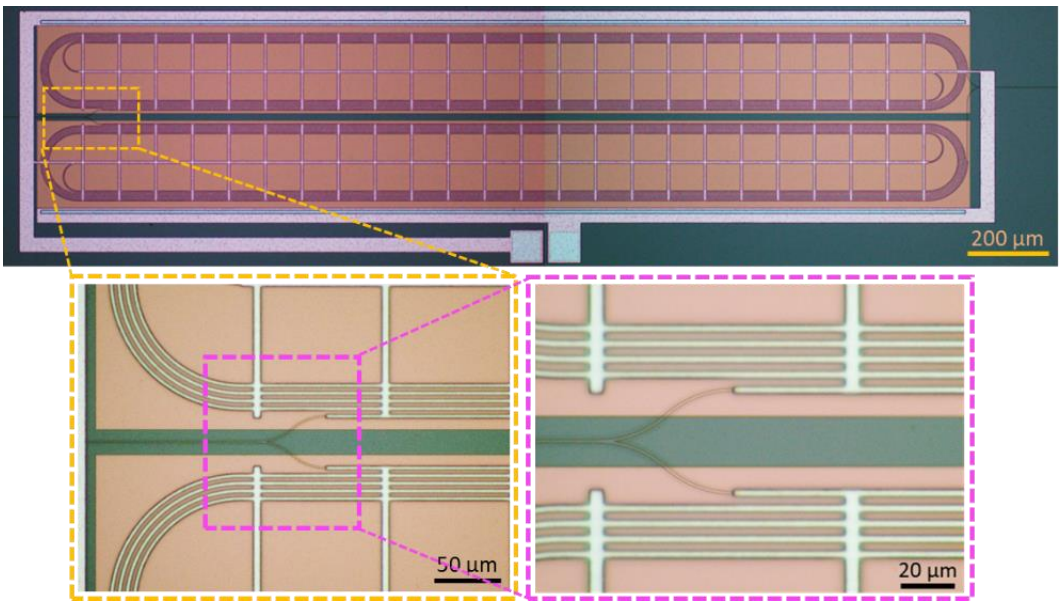

Figure S5. Optical microscope images of the long aluminum nitride (AlN) Mach-Zehnder interferometer (MZI). The details of the spiral structure are shown in the zoom-ins.

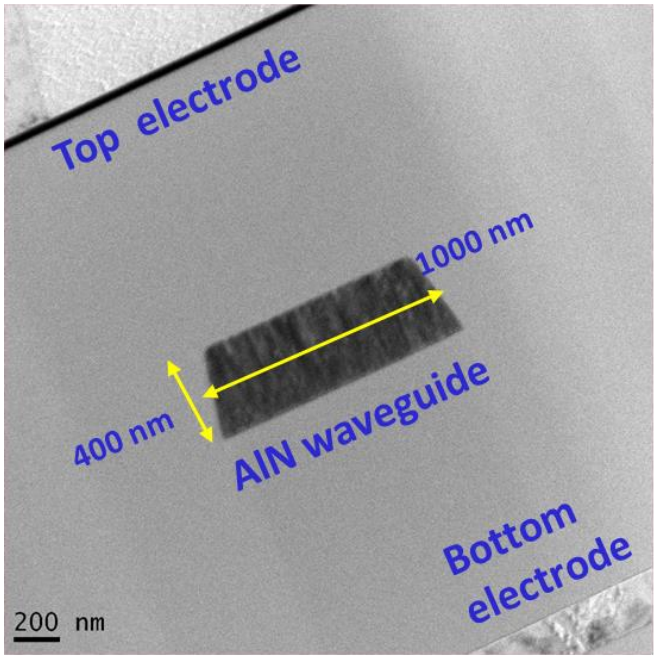

Figure S6. Tunneling electron microscope (TEM) image of the tunable aluminum nitride (AlN) waveguide's cross-section. The waveguide is sandwiched by a pair of top and bottom electrodes.

Note S3 Output power fitting of the THMIs

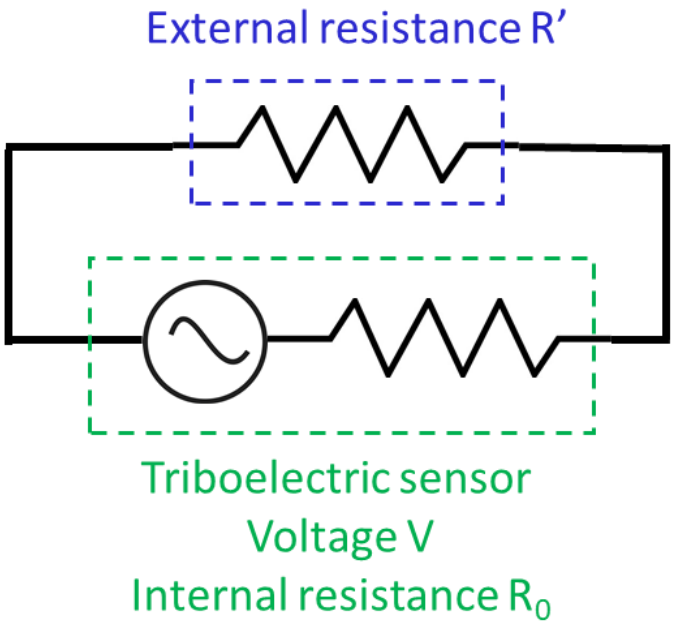

Figure S7. Equivalent circuit model diagram of the THMI connected with an external resistance.

Figure S7 shows the equivalent circuit model diagram when the THMI is connected with an external resistance. The THMI can be regarded as a voltage source V with an internal resistance R_0 while the external resistance is R'. The output power of the THMI (P) is:

$$P = \left(\frac{V}{R_0+R'}\right)^2 \times R', \qquad \text{Equation S1}$$

In the power curve presented in **Figure 2c** and **Figure 2i,** the x-axis and y-axis are R' and P respectively. Thus, fitting **Figure 2c** and **Figure 2i** using Equation S1, V, and R_0 as fitting parameters can be obtained. For the S-THMI and the T-THMI, the fitted curves are represented by $P_{S\text{-}THMI} = (77.6 / (57.3 + R')) \times 2 \times R'$ and $P_{T\text{-}THMI} = (22.7 / (65.4 + R')) \times 2 \times R'$ respectively.

Note S4 Sophisticated interferogram fitting method

If two peaks with different transmission are chosen, the curve can still be fitted well because the difference in transmission is caused by the variation of mean optical power and the fluctuation caused by fiber-to-chip coupling. Figure S8 shows the method to eliminate both factors. We take the transmission spectrum shown in Figure 3e as an example. By subtracting the mean optical power (blue) from the actual normalized transmission (red) in Figure S8a, we can obtain the transmission curve independent of the mean optical power variation, presented as the orange curve in Figure S8b. The fluctuation-induced transmission variation can be characterized by the interferogram's Hilbert transform, labeled as the green curve in Figure S8b. After subtracting the green curve from the orange curve, a transmission spectrum irrelevant to both the mean optical power variation and coupling fluctuation is obtained and plotted as the black curve shown in Figure S8c. This updated curve shows minimal transmission fluctuation and is fitted well by sine fit (cyan curve) with an R-square of 0.935. The FSR is 7.07 nm. The lower R-square value and the smaller FSR as compared to Figure 3e and Figure 3f in the main text is caused by dispersion, which will not be a problem if only two peaks are considered. Because the wavelength window is narrow and causes negligible dispersion.

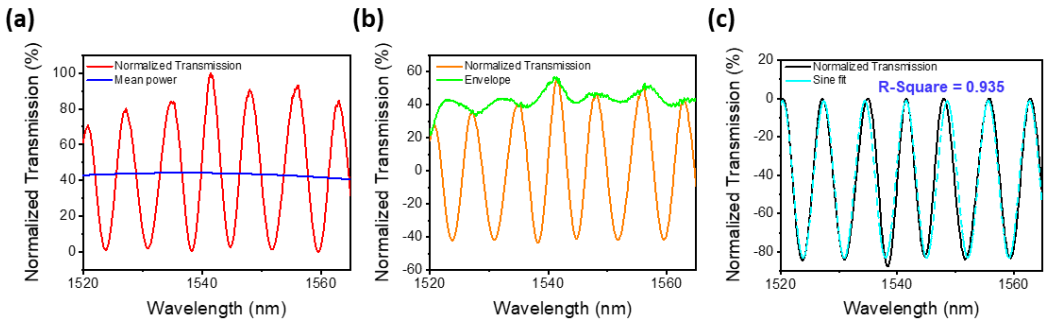

Figure S8. Interferogram fitting. (a) Original transmission spectrum with large variation. The blue curve is the mean power. (b) Transmission spectrum after subtracting the mean power from

the red curve in (a). The green curve is the absolute value of the interferogram's Hilbert transform. (c) Transmission spectrum after substracting the green curve from the orange curve in (b). The cyan curve is the sine fit result with an R-square of 0.935.

Note S5 Aluminum nitride Mach-Zehnder interferometer direct current phase modulation analysis

According to the results presented in **Figure 3**, the ratio of the MZI lengths (28.06 mm / 2.16 mm = 12.99) and the ratio of direct current (DC) phase modulation efficiencies (354 V / 27 V = 13.11) are almost equal, suggesting the proportionality between the phase change and the MZI arm length under DC biases. Theoretical analysis is implemented to confirm this experimentally observed proportionality. Assuming the lengths of the two MZI arms are L and $L+\Delta L$. At a zero bias, the phase accumulation of the two coherent light split by the Y-junction at the entrance of the MZI can be expressed respectively by:

$$\phi_1 = \frac{2\pi}{\lambda} \times n \times L, \qquad \text{Equation S2}$$

$$\phi_2 = \frac{2\pi}{\lambda} \times n \times (L + \Delta L), \qquad \text{Equation S3}$$

where λ is the operating wavelength and n is the effective refractive index of the propagating mode in the MZI. When a bias is applied, n will change by Δn to affect ϕ_1 and ϕ_2. Since a push-pull architecture is adopted in the MZI design to enhance the modulation efficiency, the resultant ϕ_1 and ϕ_2 are:

$$\phi_1' = \frac{2\pi}{\lambda} \times (n + \Delta n) \times L, \qquad \text{Equation S4}$$

$$\phi_2{}' = \frac{2\pi}{\lambda} \times (n - \Delta n) \times (L + \Delta L), \qquad \text{Equation S5}$$

The consequent phase shift is:

$$\Delta\phi = (\phi_1' - \phi_2') - (\phi_1 - \phi_2) = \frac{4\pi}{\lambda} \times L \times \Delta n + \frac{2\pi}{\lambda} \times \Delta L \times \Delta n, \qquad \text{Equation S6}$$

The last term can be ignored since it involves the product of two small values, and Equation S6 is reduced to:

$$\Delta\phi = \frac{4\pi}{\lambda} \times L \times \Delta n, \qquad \text{Equation S7}$$

Therefore, at the same applied bias that results in the same Δn, the phase change is proportional to length L of the AlN MZI arm.

Note S6 Analysis of overshoot in Figure 4g

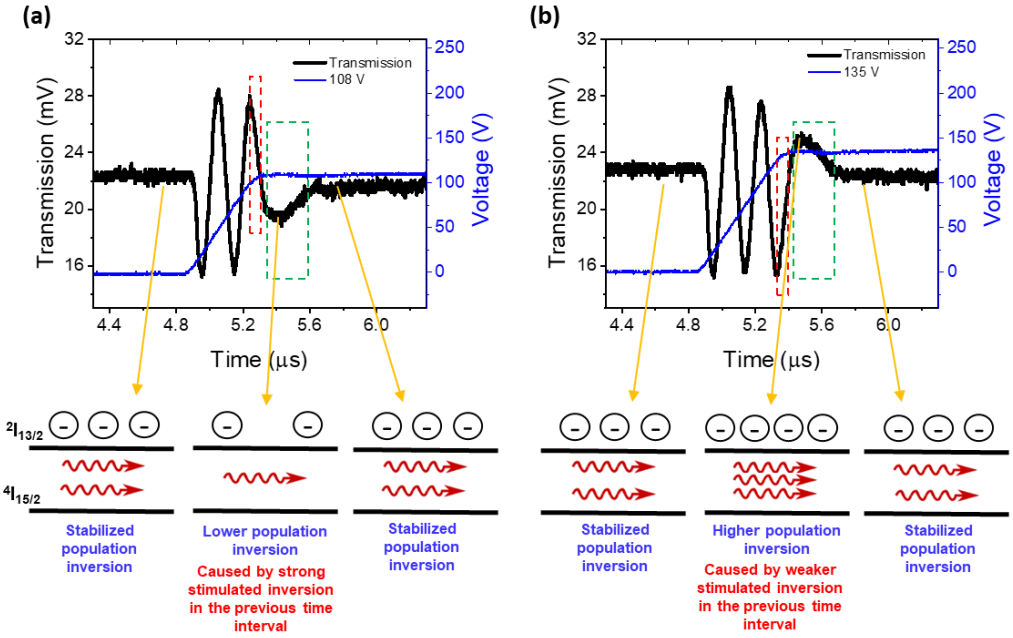

Figure S9. Analysis of overshoot in Figure 4g. (a) 4-peak scenario. (b) 5-peak scenario.

The most possible explanation is the transient gain saturation and recovery in the erbium-doped fiber amplifier (EDFA, Thorlabs, EDFA100S). The brief working mechanism of EDFA is described as the following:

When erbium is excited, the electrons jump from the $^4I_{15/2}$ energy level to the $^2I_{11/2}$ energy level and decay quickly (<10 μs) to the $^2I_{13/2}$ energy level due to phonon relaxation. The spontaneous emission time constant of the process involving the decay of electron from $^2I_{13/2}$ to $^4I_{15/2}$ is around 10 ms. This long lifetime allows population inversion for lasing. A more detailed description can be found in the related paper.[1] The amplification depends on the population inversion. At the edges of the signal, the population inversion is not stabilized, causing the transient effect (namely transient gain saturation and recovery). The transient effect has been investigated in several studies, suggesting 10-100 μs transient gain saturation and recovery time [23].

In our experimental data as shown in Figure 4g in the main text, without loss of generality, we took the scenarios of 4 peaks and 5 peaks to explain the overshoot right after the stabilization of the voltage. In the 4-peak scenario (Figure S9a), as the transmission drops from a peak immediately before the voltage stabilizes (red box), the high transmission causes stronger stimulated emission and reduces the population inversion. The reduced population inversion leads to the slight overshoot downward (green box) so that the population inversion is recovered. The 5-peak scenario can be explained similarly (Figure S9b). The transmission is rising from a though right before the voltage stabilizes (red box), causing weaker stimulated emission and leaving a higher population inversion. The higher population inversion results in the overshoot upward (green box) to stabilize the population inversion.

Note S7 Derivation of the relationship between transmission and force in the wearable THMI-nanophotonics systems

According to Equation (1) to Equation (3) in the main text, we can derive the relation between voltage (V) and force (F) as:

$$V = \frac{\sigma}{k\varepsilon}\left[D - \left(\frac{F}{K}\right)^{\frac{1}{n}}\right] + V_C, \qquad \text{Equation S8}$$

And the relation between transmission (T) and F as:

$$T = T_0 + T'\sin\left(\frac{\pi}{V_\pi} \times \left\{\frac{\sigma}{k\varepsilon}\left[D - \left(\frac{F}{K}\right)^{\frac{1}{n}}\right] + V_C - V_0\right\}\right), \qquad \text{Equation S9}$$

We first analyze the wearable S-THMI-nanophotonics system. From Figure 5(c) to Figure 5(g), we can obtain the next two boundary conditions:

$V = -16$ V, when $F = 20$ N, (Boundary condition 1)

$T = 9$ mV, when $F = 20$ N, (Boundary condition 2)

Moreover, from the fitting result shown in **Figure 2j**, we have already obtained $V_0 = 341$ V and $V_\pi = 358.85$ V.

Applying Boundary condition 1 (BC 1) and BC 2 to Equation S8 and Equation S9, we can obtain the semi-empirical T-F relation:

$$T = 9 + 0.0162T' + T'\sin\left(\frac{\pi}{358.85} \times \left\{\frac{-(16+V_C)}{D}\left[D - \left(\frac{F-20}{K}\right)^{\frac{1}{n}}\right] + V_c - 341\right\}\right), \qquad \text{Equation S10}$$

Fitting **Figure S10** using Equation S10 with F as the independent variable, T as the dependent variable, T', D, K, n as parameters, the resultant equation is presented in Equation (4) in the main text. The value of the parameters are:

T'=-18, D=136, K=5.173, n=0.375.

And the fitted curve is shown in the solid red line with an R-square of 0.94 in **Figure S10**.

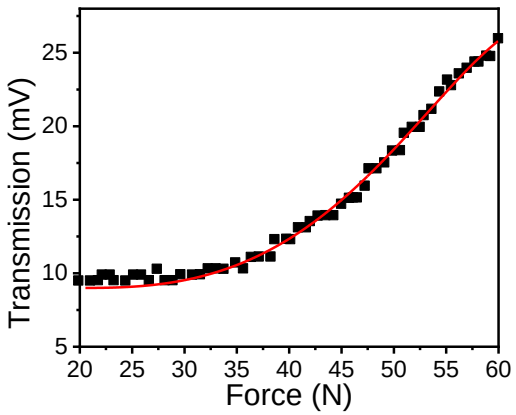

Figure S10. Measured relation between transmission and force extracted from Figure 5h. The solid red line shows the fitting result by Equation S10.

In the wearable T-THMI-nanophotonics system, the derivation process is the same. The two boundary conditions and the derived set of equations are:

$V = -30$ V, when $F = 7$ N, (Boundary condition 3)

$T = A$ mV, $when\ F = 7$ N, (Boundary condition 4)

$$T = A + 0.443T' + T'\sin\left(\frac{\pi}{26.28} \times \left\{\frac{-(30+V_c)}{D}\left[D - \left(\frac{F-7}{K}\right)^{\frac{1}{n}}\right] + V_c - 26.4\right\}\right), \quad \text{Equation S11}$$

Here, the transmission at 7 N is set as a free constant A to provide more freedom for fitting. Consequently:

The *T-F* relation and the fitted curves are presented in **Figure S11**. The resultant equation governing the *T-F* relation is presented in Equation (5) in the main text. The value of the parameters are:

A=29.342, T'=-10.708, D=18.489, K=11.828, n=0.769.

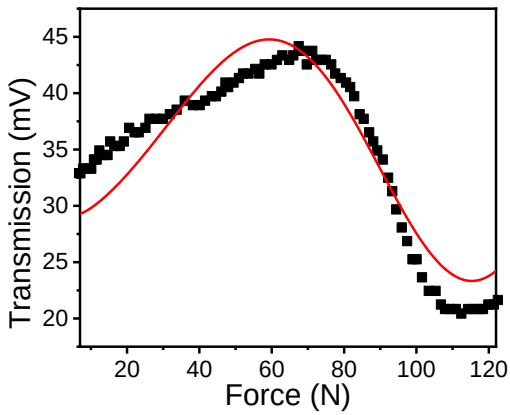

Figure S11. Measured relation between transmission and force extracted from Figure 6h. The solid red line shows the fitting result.

Note S8 Circuit diagram adopted in the augmented reality application

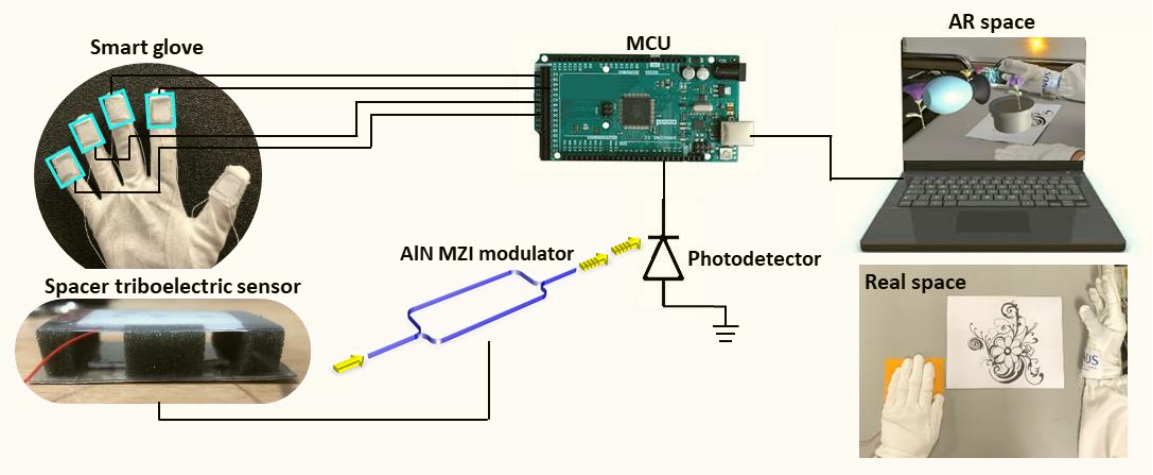

Figure S12. Circuit diagram adopted in the augmented reality application.

Reference

(1) Ono, H.; Yamada, M.; Kanamori, T.; Sudo, S.; Ohishi, Y. 1.58-Mm Band Gain-Flattened Erbium-Doped Fiber Amplifiers for WDM Transmission Systems. *Lightwave* **1999**, *17*, 490–496.

(2) Giles, C. R.; Simpson, J. R.; Desurvire, E. Transient Gain and Cross Talk in Erbium-Doped Fiber Amplifiers. *Opt. Lett.* **1989**, *14*, 880–882.

(3) Meena, D.; Sarath, K. T.; Francis, F.; Dipin, E.; Srinivas, T. Mitigation of EDFA Transient Effects in Variable Duty Cycle Pulsed Signals. *Def. Technol.* **2019**, *15*, 276–281.